iScience

CellPress
OPEN ACCESS

Article

GhUBX controlling helical growth results in production of stronger cotton fiber

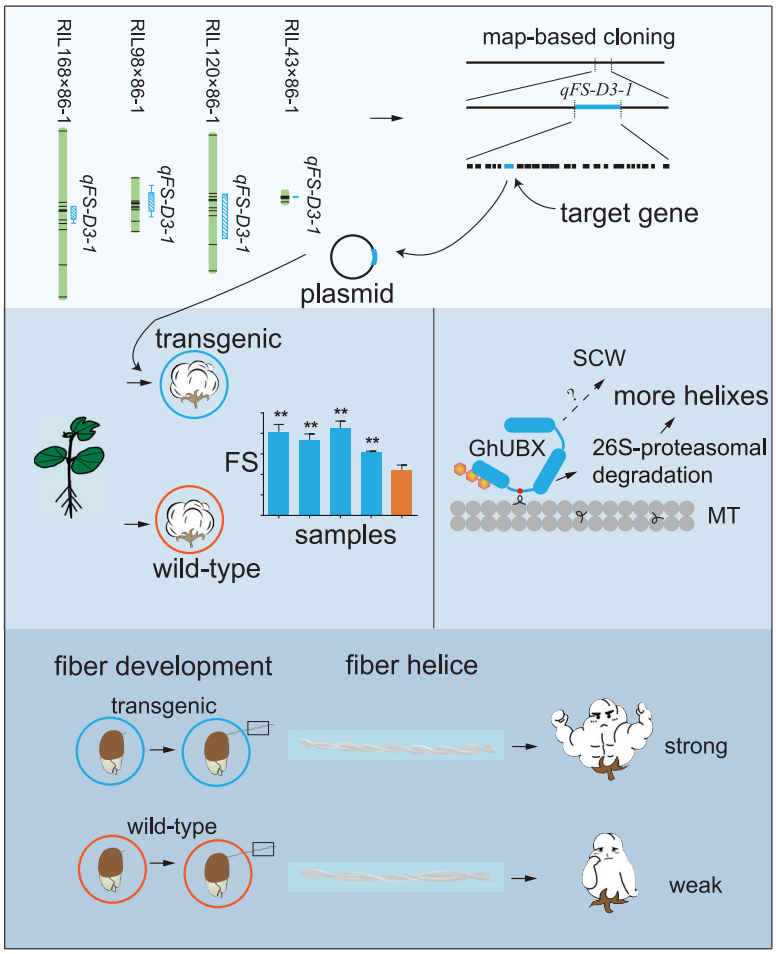

Yihao Zang, Yan Hu, Chenyu Xu, ..., Yayao Zhang, Lei Fang, TianZhen Zhang

cotton@njau.edu.cn

Highlights

Isolation of the first fiber strength gene GhUBX using map-based cloning strategy

Verification of the function of GhUBX experimentally in transgenic cotton

Link helices to the cotton fiber strength, that more helices make fiber stronger

An ubiquitin–proteasome system regulating the development of cotton fiber

Zang et al., iScience 24, 102930
August 20, 2021
https://doi.org/10.1016/j.isci.2021.102930

iScience

CellPress
OPEN ACCESS

Article

GhUBX controlling helical growth results in production of stronger cotton fiber

Yihao Zang,[1,2] Yan Hu,[2] Chenyu Xu,[1,2] Shenjie Wu,[3] Yangkun Wang,[1] Zhiyuan Ning,[1] Zegang Han,[1] Zhanfeng Si,[2] Weijuan Shen,[1] Yayao Zhang,[2] Lei Fang,[2] and TianZhen Zhang[1,2,4,*]

SUMMARY

Cotton fiber is an excellent model for studying plant cell elongation and cell wall biogenesis as well because they are highly polarized and use conserved polarized diffuse growth mechanism. Fiber strength is an important trait among cotton fiber qualities due to ongoing changes in spinning technology. However, the molecular mechanism of fiber strength forming is obscure. Through map-based cloning, we identified the fiber strength gene *GhUBX*. Increasing its expression, the fiber strength of the transgenic cotton was significantly enhanced compared to the receptor W0 and the helices number of the transgenic fiber was remarkably increased. Additionally, we proved that GhUBX regulates the fiber helical growth by degrading the GhSPL1 via the ubiquitin 26S–proteasome pathway. Taken together, we revealed the internal relationship between fiber helices and fiber stronger. It will be useful for improving the fiber quality in cotton breeding and illustrating the molecular mechanism for plant twisted growth.

INTRODUCTION

Helical growth is a widespread phenomenon in the plant kingdom. It is seen in the coiling of tendrils, reversal growth of buds and leaves, spiraled arrangement of petals, and twisting of leaf blades. There are many examples of helical growth in plants, not only in the tendrils of climbing plants such as the grapevine *Vitis vinifera* and the pedicels of orchid buds (e.g., the *Cattleya* hybrid, family Orchidaceae) but also in the petals of *Lagunaria patersonia* (family Malvaceae) and leaves of the geebung shrub *Persoonia helix* (family Proteaceae) (Jaffe and Galston, 1968; Smyth, 2016). Generally, the shape and movement of plants are determined by the directional expansion of cells, which is caused by the interaction between the cell turgor pressure and cell wall tension (Skotheim and Mahadevan, 2005; Dumais and Forterre, 2012). The spatial distribution of cell wall microfibers determines the polarity of the cell expansion shaping the plant form. Multiple recent studies have highlighted the fact that the cortical microtubules play an important role in microfibril orientation. For instance, membrane-assisted cortical microtubules regulate the arrangement of cellulose microfibers (Tiwari and Wilkins, 1995; Baskin, 2005; Paredez et al., 2006). The microtubule and actin cytoskeletons cooperate to influence shape change in plant cells (Yanagisawa et al., 2015). In most situations, the helical growth of plant cells is associated with rearrangement of cortical microtubules. These helical rearrangements have been proposed to drive the handedness of cell elongation (Ishida et al., 2007).

Allotetraploid upland cotton (*Gossypium hirsutum* L.) is the leading natural fiber-producing species, accounting for 95% of cotton production worldwide. Cotton fiber cells show twisted growth as they grow. Li et al. (2009) reported that the overexpression of fibroin, a silkworm gene, could increase fiber helices. Fiber strength (FS) refers to the ability of a fiber to withstand a load before breaking. It not only depends on the amount of cellulose contained in cell walls (a higher percentage of strength is attributed to greater rigidity of cellulosic chains) but also on the frequency and distribution of reversal and convolutional structures in the microfibril helix (Hsieh, 1999; Haigler, 2010). In recent yr, the improvement of fiber quality has been driven primarily by the advent of high-speed rotor spinning. The convolutional structure could increase the binding force between the fibers and improve the yarn strength during high-speed rotor spinning.

Until now, several hundred quantitative trait loci (QTLs) related to fiber quality traits (e.g., fiber strength, length, uniformity, micronaire) have been mapped using various of genetic segregated populations (Zhang et al., 2003; Mei et al., 2004; Rong et al., 2007; Lacape et al., 2010). However, pinpointing the exact location

[1]State Key Laboratory of Crop Genetics and Germplasm Enhancement, College of Agriculture, Nanjing Agricultural University, Nanjing 210095, China

[2]Agronomy Department, College of Agriculture and Biotechnology, Zhejiang University, Hangzhou 310029, China

[3]Biotechnology Research Center, Shanxi Academy of Agricultural Sciences, Taiyuan 030031, China

[4]Lead contact

*Correspondence: cotton@njau.edu.cn

https://doi.org/10.1016/j.isci.2021.102930

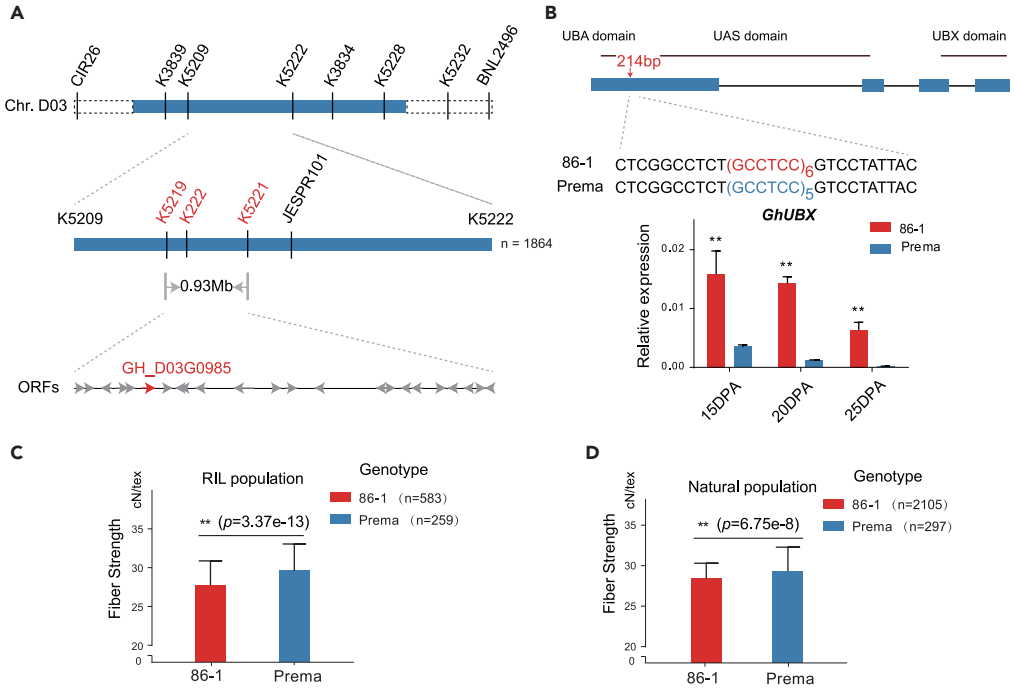

Figure 1. Cloning of *qFS-D3-1*

(A) *qFS-D3-1* was mapped on the D3 chromosome between the k5209 and k5222 markers using an F_2 generation. *qFS-D3-1* was further fine-mapped to a region between the K5219 and K5221 markers using 1864 individuals. The mapping area was narrowed down to a 0.93-Mb genomic interval, and *GH_D03G0985* (*GhUBX*) was selected as a major gene.

(B) GhUBX contains 4 exons and 3 introns. The DNA sequence alignment of the *GhUBX* gene exhibits a 6-bp difference between Prema and 86-1.

(C and D) Genotype association analysis of the k222 marker for fiber strength in RILs and natural populations. 86-1: 86-1 genotype (GCCTCT(GCCTCC)$_6$GTCC), Prema: Prema genotype (GCCTCT(GCCTCC)$_5$GTCC); p values were determined by the Student's t-test (**, $p < 0.01$).

of genes with a large effect underlying the QTL is still a mammoth task. To our knowledge, map-based cloning of the exact gene conferring the QTL in cotton has not been reported. In this study, we cloned a causal gene, *GhUBX*, responsible for higher FS using map-based cloning of a major-effect QTL, *qFS-D3-1*. The GhUBX reduces the content of the GhSPL1 protein in fiber cells via the ubiquitin 26S–proteasome pathway; it acts as the bridge between ubiquitin and the plant-specific microtubule-associated protein GhSPL1. Increased *GhUBX* transcripts could significantly increase the fiber helices and, consequently, improve the FS of transgenic cotton.

RESULTS

Map-based cloning of the FS QTL *qFS-D3-1*

The major-effect QTL for FS, named *qFS-D3-1*, originated from Prema and was mapped on chromosome D03 (Chr. D03) (Figure 1A). It could be identified simultaneously in four environments with a phenotypic variation ranging from 2.11% to 14.71% with substantially high logarithm-of-the-odds (LOD) scores that fluctuated from 5.46 to 14.58 (Ning et al., 2014). To finemap and clone this QTL, four recombinant inbred lines (RILs), RIL43, RIL98, RIL120, and RIL168, that derived from (Prema × 86-1) RILs and contained the common *qFS-D03-1* locus, were backcrossed with 86-1, respectively, to produce four secondary mapping populations (Figures S1A and S1B and Table S2). The *qFS-D3-1* was detected in these four F_2 populations and anchored within a 23.5-centimorgan interval with six pairs of single-nucleotide polymorphisms (SNPs) and three pairs of insertion-deletion (InDel) markers (Figure S1C). Using the newly developed simple sequence repeats (SSRs), SNPs, and InDel markers in this interval (Wang et al., 2015), we delimited the *qFS-D3-1* within a 1.14-cM interval between markers K5219 and K5221 with an LOD of 15.54 using the segregating (four RILs × 86-1) F_2 comprised 1,864 individuals (Table S3), corresponding to a 0.93-megabase (Mb) physical distance on Chr. D03. Based on our updated genome sequence of *G. hirsutum* acc. TM-1 (Hu et al.,

2019), 23 genes had been annotated in this short region (0.93 Mb) (Table S4). Transcriptomic data (https://cotton.zju.edu.cn) showed that 11 of 23 candidate genes were expressed during the stages of fiber development and confirmed by the real-time quantitative polymerase chain reaction (qRT-PCR) (Figures S1D and S2A). Among these 11 genes, five showed differential expression in just one fiber development stage between Prema and 86-1, and one gene (*GH_D03G0985*) always showed a lower expression in the fibers of Prema than those of 86-1 (Figure S2A). The full-length coding regions of the six differentially expressed genes from Prema and 86-1 were isolated and sequenced. Sequence alignment indicated that five genes differentially expressed in just one fiber development stage had the same protein sequence between Prema and 86-1. However, we detected a 6-bp (GCCTCC) SSR variation conferring the deletion of two amino acids (Ala-Ser) at the N-terminal of *GH_D03G0985* (Figure 1B) in Prema compared with 86-1. Therefore, *GH_D03G0985*, annotated as a UBX (*GhUBX*), was the candidate gene for *qFS-D3-1*.

The SSR in *GhUBX* has a significant correlation with the FS trait

Sequence alignment showed that the haplotype of *GhUBX* gene was classified into the *GhUBX*-Prema type, with CTCGGCCTCT $(GCCTCC)_5$, and the *GhUBX*-86-1 type, with CTCGGCCTCT $(GCCTCC)_6$. The SSR marker K222 was designed surrounding this SSR variation. The 183 RILs derived from (Prema × 86-1) were divided into two major categories by the marker K222, *GhUBX*-Prema and *GhUBX*-86-1 (Figure 1C and Table S5). Their association analysis showed that the 6-bp variation in the SSR region was cosegregated with an FS trait under different field conditions in multiple years at five different locations, including Shihezi, Xinjiang province, the most important cotton production area in China (Figure S2B).

The haplotype association studies of 268 cotton cultivars (Fang et al., 2017) with marker K222 also showed an extremely significant association with an FS trait at Korla, Xinjiang province (p value = 3.13×10^{-4}, Student's test), Nanjing, Jiangsu province, and Anyang, Henan province, three cotton-growing regions in China (Figures 1D and S2C). The accessions with Prema-type *GhUBX* haplotypes had stronger FS than that of the 86-1 type accessions. Of the examined accessions, 87.7% (n = 235) had the 86-1 genotype and only 12.3% (n = 33) contained the Prema genotype (Table S6). This suggests that this elite allelic variation have a huge potential for improving the FS in cotton breeding in the future.

The full CDS length of the *GhUBX* was 1416 bp in the 86-1 type and 1410 bp in the Prema type (Figure S2D). The protein contained an ubiquitin-associated (UBA) domain in the N-terminal, an ubiquitin-associating (UAS) domain in the middle. and an ubiquitin regulatory X (UBX) domain in the C-terminal, consistent to other UBX family proteins (Deruyffelaere et al., 2018). The SSR repeat region containing the 6-bp InDel mentioned above was not located within any known domains (Figure S2E). *GhUBX* was consistently expressed in all the tested tissues, including roots, stems, leaves, and fibers at different developmental stages, and its expression was significantly lower in the fibers of Prema than those of 86-1 (Figure S2F).

GhUBX is associated with the fiber helix

To gain further insight into the biological role of *GhUBX* in determining the FS, we developed a total of 12 independent *GhUBX*-overexpression (OE) transgenic lines through the *Agrobacterium*-mediated transformation method (Wu et al., 2008). According to PCR detection and expression level of *GhUBX* by qRT-pCR, four *GhUBX*-OE lines (designated as OE-120, OE-141, OE-145, and OE-153) with a noticeably increased expression level of the *GhUBX* were selected and successively self-pollinated to develop pure lines for further analysis (Figures 2A and S3A). The FS parameter (cN/tex: centi-Newton per tex) was increased in the transgenic *GhUBX*-OE lines by 24.0%, compared with the receptor W0 (Figure 2B and Table S7). Correspondingly, we examined the thickness of cell wall and the number of helix per unit length in the transformed and untransformed cotton lines. Compared with the transgenic receptor W0, the fiber helix number per unit length was increased by 93.2%, the secondary cell wall (SCW) was reduced by 11.71%–23.83% in the *GhUBX*-OE lines (Figures 2C–2F, S3B, and S3C). The variation trend of the helix number per unit length was consistent with FS. Therefore, we theorized that the fiber helices might be closely related to the FS. Moreover, both right- and left-handed helices were presented in mature fibers (Figure 2C), indicating that handedness was a randomly selected trait. These phenomena in natural cotton cultivar population were further validated. We selected 60 cultivars with extremely higher and lower FS from the worldwide cotton cultivars to measure the number of fiber helix. A positive relationship between fiber helix and strength was found, and the cultivars with higher FS contained more helices (Figure S4 and Table S8). These results suggested incensement of the helix number per unit could enhance fiber elasticity, thereby improving the resistance ability of fibers against external pulling forces and stress (Hsieh, 1999; Haigler, 2010).

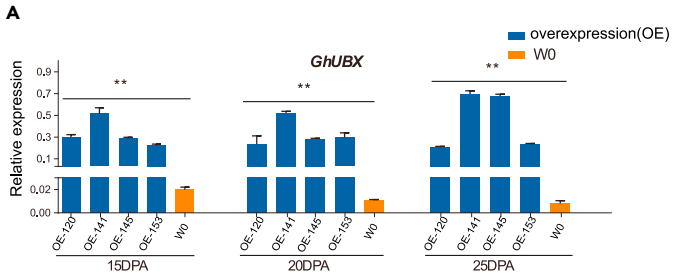

B

year / sample	2018 Dangtu	2019 Sanya	2019 Dangtu
W0	28.35 ± 0.56	23.10 ± 0.44	29.25 ± 0.35
OE-120	30.61 ± 0.71	25.37 ± 0.77*	33.33 ± 0.33**
OE-141	31.07 ± 0.59*	27.28 ± 1.24*	36.27 ± 1.37**
OE-145	31.00 ± 0.48*	27.97 ± 1.10**	34.07 ± 1.11**
OE-153	30.71 ± 0.54*	25.47 ± 0.72*	32.63 ± 0.26**
Prema	31.06 ± 1.02	27.73± 0.75	36.77 ± 1.76
86-1	25.48± 1.41	22.20± 0.46	27.67± 1.21

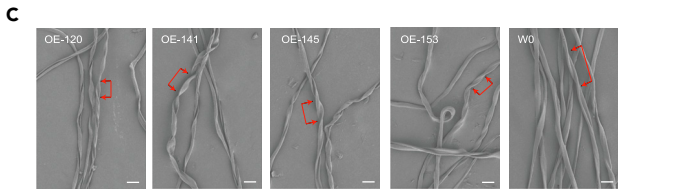

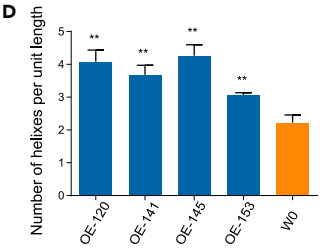

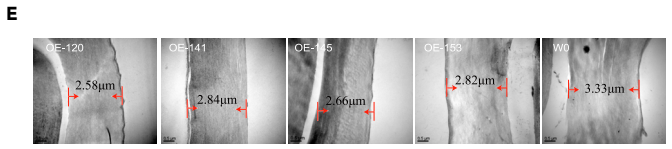

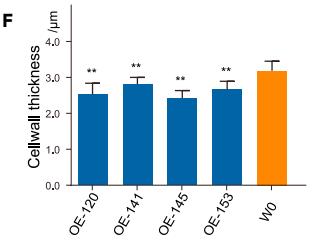

Figure 2. Transgenic validation of GhUBX conferring increase of fiber strength

(A) qRT-PCR analysis of *GhUBX* expression in fibers of the receptor W0 and the *GhUBX*-OE at 15, 20, and 25 DPA. *Histone3* was used as the internal control.

(B) Comparison of fiber strength (cN/tex: centi-Newton per Tex) parameters between the W0 and transgenic cotton plants for three seasons, with three replicates for each sample.

(C) Scanning electron microscopy (SEM) of W0 and transgenic mature fibers (OE-120, OE-141, OE-145 and OE-153). Scale bars on the SEM images are 50 μm.

(D) Measurement of the helix numbers by SEM in the W0 and transgenic cotton lines; total length of each mature fiber was over 15 cm. n > 30.

(E) Transmission electron microscopy (TEM) of the W0 and transgenic mature fibers (OE-120, OE-141, OE-145 and OE-153); scale bars on the TEM images are 0.5 μm.

(F) Cell wall thickness of mature fiber in the W0 and transgenic lines. The data in A, B, D, and F are shown as the mean (±SD) of three experimental replicates; p values were determined by the Student's *t*-test (*, $p < 0.05$; **, $p < 0.01$).

Short tandem repeat variations influence the interaction of GhUBX with GhSPL1

To address the molecular basis of fiber helix regulation by *GhUBX*, yeast two-hybrid (Y2H) assay was performed to identify its interacting proteins (Table S9). We detected a strong interaction of GhUBX with ubiquitin 10 and SPIRAL1-like1. It has been reported that UBX is involved in protein degradation, so its interaction with ubiquitin 10 is within our expectation. Therefore, we paid more attention to another interacting protein, SPIRAL1-like1. *SPIRAL1-like1* encodes a six-member family gene, sharing an amino acid homology of 60% with the *SPIRAL1* gene in *Arabidopsis*, so we named it *GhSPIRAL1-like1* (*GhSPL1*). As previously reported (Sedbrook et al., 2004; Nakajima et al., 2004; Wang et al., 2011; Shoji et al., 2004), the *SPIRAL1* gene functions as a plant-specific microtubule-associated protein (MAP) and regulates the helical growth of roots. The interaction between GhUBX and GhSPL1 was double-checked by coimmunoprecipitation (co-IP) and pull-down assays *in vitro* (Figures 3A and 3B), by bimolecular fluorescence complementation (BiFC) assays (Qin et al., 2019), and firefly luciferase complementation imaging (LCI) in *planta* (Figures 3C and 3D). Strong fluorescence signals in the cortical microtubules were observed in *Arabidopsis* protoplasts and *Nicotiana benthamiana* leaves, indicating that GhUBX and GhSPL1 were colocalized with the microtubule marker MAP-65 (Figures S5C and S5D). Their subcellular location inferred that GhUBX interacted with GhSPL1 directly in the cortical microtubules of the developing fibers.

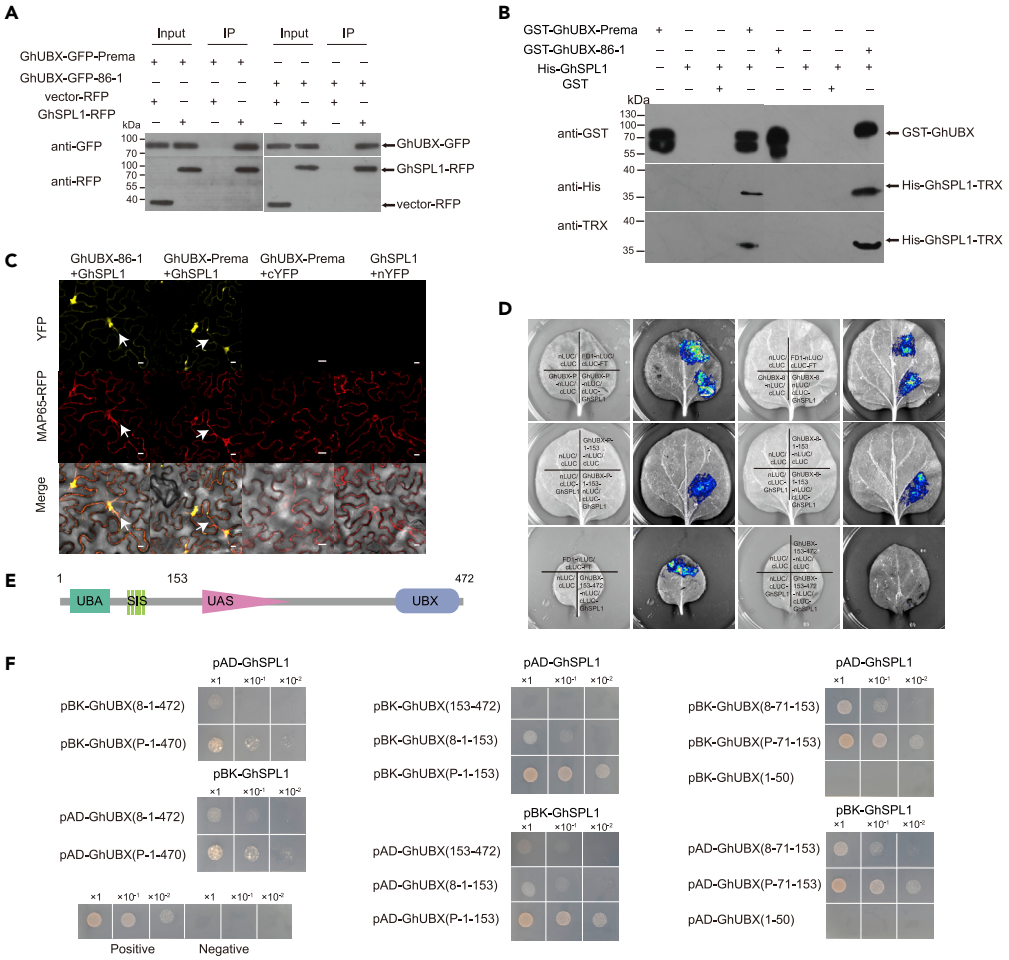

Figure 3. GhUBX interaction with GhSPL1

(A) GhUBX from Prema and 86-1 can interact with GhSPL1 in a co-IP assay. Co-IP was carried out with anti-GFP agarose from total isolated proteins, and immunoblotting analysis was done with anti-GFP and anti-RFP antibodies.

(B) The direct interaction between GhUBX and GhSPL1 tested with the *in vitro* pull-down assay.

(C) The interaction of GhUBX and GhSPL1 confirmed by the BiFC assay in *N. benthamiana*. *MAP-65-RFP* as a marker for microtubule localization was cotransformed. Scale bars = 10 μm.

(D) GhUBX (1–153), but not GhUBX (153–472), can interact with GhSPL1 as indicated by the split firefly luciferase complementation imaging assay.

(E) The domain composition of GhUBX amino acid sequence: UBA (ubiquitin-associated domain); SIS (SPL1 interacting site); UAS (ubiquitin-associating domain); UBX (ubiquitin regulatory X domain).

(F) Y2H assays to investigate the interaction between different domains of GhUBX and GhSPL1. N-terminal amino acids 71 to 83 of 86-1 and 71 to 81 of Prema contribute to the interaction with GhSPL1. Deletion of two amino acids in aligning amino acid sequences caused the differences in interactions between GhUBX and GhSPL1. pGBKT7-*p53* and pGADT7-*T-antigen* were used as positive controls, and pGBKT7-*Lamin c* and pGADT7-*T-antigen* as negative controls.

To test the exact binding region between GhUBX and GhSPL1, GhUBX was divided into several parts to perform the Y2H assay and LCI assay. The Y2H results showed that GhUBX (71–153) was responsible for its interaction with GhSPL1 (Figures 3E and 3F). Further, Y2H and LCI assays revealed that the N-terminal amino acids from the 71st to the 81st regions (in Prema) or to the 83rd region (in 86-1) within the SSRs in GhUBX contributed to its interaction with GhSPL1 (Figures 3D and 3F). Overall, these results indicated that this SSR region was the key site bonding with GhSPL1, so we named it as Gh**S**PL1 **I**nteracting **S**ite (**SIS**) domain. In addition to the UBA, UBX, and UAS domains previously reported (Deruyffelaere et al., 2018), a novel SIS domain bound by SPIRAL1-like 1 is identified in the *GhUBX* gene.

In *Arabidopsis*, *SPIRAL1*(*SPR1*) was reported to be involved in twisted growth, and loss of SPR1 function conferred right-handed twisting of the plant axis, including the roots, stems, and leaves (Sedbrook et al., 2004; Nakajima et al., 2004). There are two *SPIRAL1-like 1* orthologs in Upland cotton, *GH_D03G1112* (*GhSPL1*) and *GH_A03G0847* (*GhSPL1-A*). To explore its orthologous function, virus-induced gene silencing (VIGS) assay was used. Young leaves twisted in the *GhSPL1*-downregulated VIGS cotton plants (Figures S6A–S6C). At the boll opening stage, we harvested the mature fiber of *GhSPL1*-silenced group and TRV:00 plants (CK), while both FS and helix number were significantly enhanced in *GhSPL1*-downregulated plants than CK (Figures S6D and S6E and Table S10). Ectopic expression of *GhSPL1* in the *spiral1* mutant lines: CS6546 and SALK_048697, which displayed helical growth phenotypes in the roots of plants (Nakajima et al., 2004), rescued the helical growth of root epidermal cells in *Arabidopsis*, consequently, they became normal, just as the wild type (Figures S7A–S7C), that further confirmed the orthologous role of this gene in regulating twisted growth in plants.

GhUBX could bridge ubiquitin to GhSPL1 via its UBA domain and SIS domain

Several UBX-containing proteins form a bridge for ubiquitin with substrate proteins in yeast (Lee et al., 2017; Neuber et al., 2005; Schuberth and Buchberger, 2005). We identified the same interaction of GhUBX with the conserved ubiquitin and its UBA domain by Y2H assay (Figures S8A and S8B). Through the combination of a prey constructed expressing ubiquitin, a bait constructed expressing GhSPL1 and sectionalized GhUBX bridge proteins (Figure 4A), the interactions among GhUBX, GhSPL1, and ubiquitin were detected by Y3H assay. Yeast cells cotransformed with pGADT7-ubiquitin and pBridge-P, pBridge-8, pBridge-NP, pBridge-N8, and pBridge-C grew in the SD/-Leu-Trp medium but not in the SD/-Leu-Trp-His-Ade medium (Figure 4B), indicating that ubiquitin did not interact with GhSPL1. When the mentioned yeast cells were spotted on the SD/-Leu-Trp-His-Met medium, they could grow well, except for pGADT7-ubiquitin and pBridge-C (Figure 4B), indicating that GhUBX is the bridge between GhSPL1 and ubiquitin, and the SIS domain in the N-terminal of GhUBX acts as a key player in the binding of GhUBX to GhSPL1.

GhUBX could degrade GhSPL1 via the ubiquitin 26S–proteasome pathway

In vitro assays using purified GST-GhUBX and His-GhSPL1 proteins, GhSPL1 could be ubiquitinated in the presence of E1, E2, and GhUBX proteins (Figure 4C), the ubiquitination of GhSPL1 by GhUBX promoted its complex degradation. Also, GhSPL1 was degraded by 26S–proteasome pathway. When GhUBX and GhSPL1 both existed with MG132 (a 26S-proteasome-specific inhibitor), the signals could be detected with antibody RFP and antibody GhSPL1 due to the degradation mediated by GhUBX could be suppressed by MG132 (Figure 4D). The more GhUBX led to the decreased of GhSPL1 in developing fiber of Prema, which was opposite in 86-1 (Figures S8C–S8E). This degradation was further proved by semi-*in vivo* degradation assays that GhUBX-Prema could degrade GhSPL1 faster than GhUBX-86-1 (Figure 4E). Furthermore, the overexpression of *GhUBX* significantly decreased the content of GhSPL1 in developing fibers (Figure S9). All these results revealed that GhUBX could regulate the fiber helix in a complex regulatory pathway. In this complex, GhUBX, serving as a functional E_3 ligase, makes effect as the bridge between ubiquitin and GhSPL1 via its UBA and SIS domains, and the GhSPL1 is ubiquitinated and further degraded via the ubiquitin 26S-proteasome-dependent pathway (Figure 5). The reduced GhSPL1 contents lead to the increment of the fiber helices by regulating the stability of the microtubules and, hence, influencing the FS of the transgenic cotton.

DISCUSSION

GhUBX regulates cotton FS by helix

FS is attributed to the rigidity of the cellulosic chains, the frequency and distribution of the reversal, convolutional structure of the microfibril helix and orientation and other characteristics (Hsieh, 1999). Until now, there have been many studies on the influence of SCW on FS. A large number of genes, such as *TALE* superfamily genes, *GhXLIM6*, *GhKNL1*, and *GhCesA4*, and transcription factors, including *MYB*, *NAC*, and *GhTCP4*, have been reported as probably being involved in SCW thickening (Huang et al., 2019; Zhang et al., 2018; Sun et al., 2020; Ma et al., 2019; Li et al., 2018; Gong et al., 2014; Cao et al., 2020). However, the FS is a comprehensive trait not only depending on the thickness of SCW but also convolutional structure of the microfibril helix and orientation and other characteristics (Hsieh, 1999). The ubiquitin–proteasome system has been explored extensively including autophagy, nuclear transport of specific proteins, repair of DNA, and a multitude of signal transduction pathways (Varshavsky, 2017). Protein with UBX domain, serving as a functional E3 ligase in the ubiquitin–proteasome system, participating in lipid droplet formation and

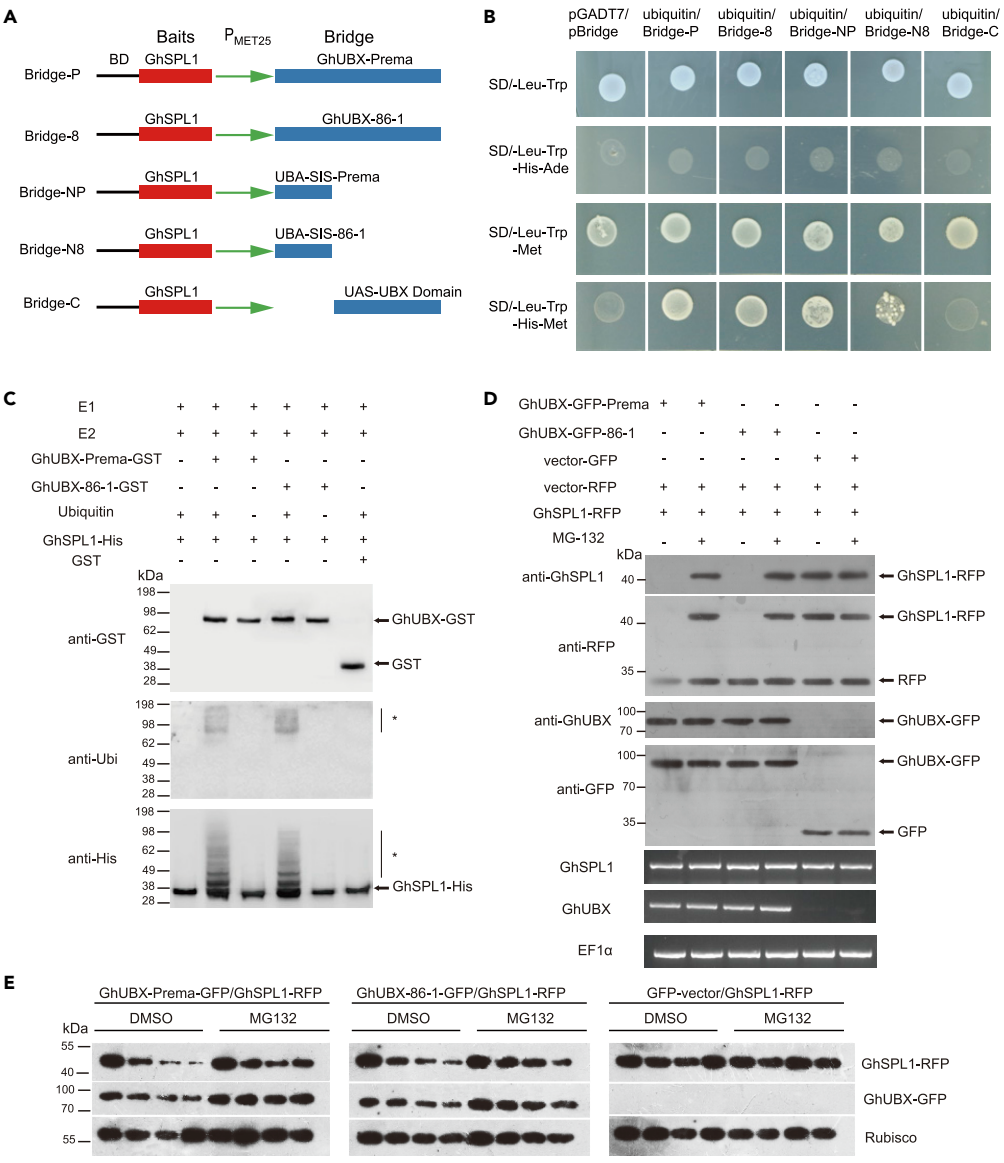

Figure 4. Degradation of a complex ubiquitin/UBX/SPL1 molecule via ubiquitin 26S-proteasome pathway

(A) The constructs expressing both the bait and bridge proteins for Y3H assays.

(B) GhUBX acts as a bridge between ubiquitin and GhSPL1 in Y3H interactions. Ubiquitin did not interact with GhSPL1 directly, but GhUBX (UBA and SIS domain), ubiquitin and GhSPL1 showed interactions.

(C) GhUBX ubiquitinates GhSPL1 *in vitro*: ubiquitinated GhSPL1-His was detected by anti-ubiquitin and anti-His. * indicates ubiquitinated GhSPL1.

(D) GhUBX promotes the degradation of GhSPL1 via the 26S-proteasome *in vivo*. Immunoblotting analysis of protein extracts corresponding to agroinfiltrated *N. benthamiana* leaves with the indicated plasmids in the presence or absence of MG132. Immunoblotting analysis was done with anti-GFP and anti-RFP antibodies. The anti-RFP antibody served as a loading control. The mRNA expression levels of GhUBX and GhSPL1 were analyzed by RT-PCR, and the mRNA expression level of *EF1α* was used as the internal control.

(E) GhUBX promotes the degradation of GhSPL1 in a semi-*in vivo* protein degradation assay. Extracts from GhSPL1-RFP were mixed together with GhUBX-Prema-GFP, GhUBX-86-1-GFP or GFP-vector, after which the mixtures were treated with CHX and ATP in the presence of MG132 or DMSO for different times. GFP antibody and RFP antibody were used for detecting the abundance GhUBX and GhSPL1. Rubisco was used as a loading control.

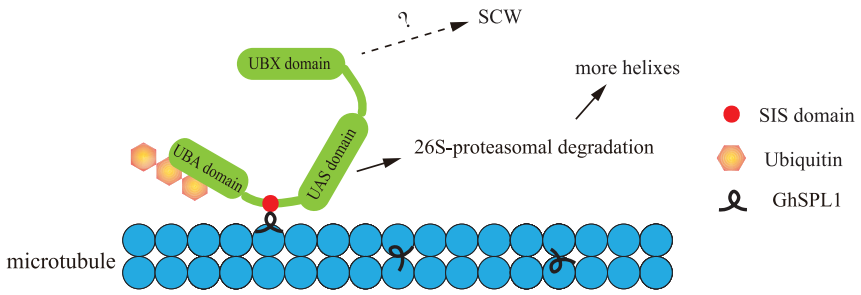

Figure 5. A working model of GhUBX ubiquitinates GhSPL1 via ubiquitin 26S-proteasome pathway

In the working model, GhUBX is a bridge protein that functions by bonding to ubiquitin and GhSPL1 via its UBA domain and SIS domain, respectively. GhUBX recruits GhSPL1 for degradation via the ubiquitin 26S-proteasome pathway. In transgenic cotton, overexpression of GhUBX reduces the GhSPL1 protein in microtubule, leading to more helices in mature fibers.

degradation of lipid droplet proteins (Wang et al., 2011; Zhang et al., 2017; Feng et al., 2018; Kretzschmar et al., 2018). The role of UBX protein in controlling FS has not yet been elucidated. In this study, one new gene containing a UBX domain was identified in two cotton cultivars, Prema and 86-1 (Figure 1). The role of GhUBX, a functional E_3 ligase, has been suggested in the ubiquitination and degradation of GhSPL1 via the ubiquitin 26S–proteasome-dependent pathway (Figure 4). The N-terminal of GhUBX has a short tandem repeat variation as the SIS domain, which plays a vital role in binding protein GhSPL1 (Figure 3). The GhUBX-OE lines have less GhSPL1 content in the developing fiber cell, leading to the enhancement of the fiber helix compared with the wild type (Figures S6 and S9). In general, *GhUBX*-OE lines have thinner SCW than W0, whereas the improvement of FS in the *GhUBX*-OE lines is contributed mostly by more helices. It is amazing, but it makes sense. As for the helices, it is easy to imagine that more helices could enhance the FS (Martinez-Sanz et al., 2017). More helix enhance fiber elasticity due to the improved resistance to external pulling forces, the effects of helix rescue the adverse effect of the reduction of SCW.

SPIRAL1 is one of the first proteins identified that determines the twisted growth of plants (Sedbrook et al., 2004; Nakajima et al., 2004). It is a key dynamic microtubule-based modulator for helical growth (Galva et al., 2014). Recent research has confirmed that SPIRAL1 could bind to microtubules and regulate their stability, the spatial distribution of cell wall microfibers could influence the polarity of cell expansion (Wang et al., 2011). Membrane-assisted cortical microtubules guide the arrangement of cellulose microfibers (Paredez et al., 2006), thus affecting the cell twisting in fiber development (Sambade et al., 2014). The arrangement of fibrils on the surface of fibers at the secondary synthesis stage could influence fiber quality (Han et al., 2013). Recent research has confirmed the actin and microtubule cooperate to pattern the cell wall and growth (Yanagisawa et al., 2015). The arrangement of fibrils affects not only thickness of SCW but also helix of fiber. We suggest here that the differential expression of *GhUBX* in fibers at the SCW synthesis stage between two parents finally influences the helicity of mature fibers. The increased helices in fiber can make fiber stronger in the GhSPL1-silencing group than the CK group (Figure S6 and Table S10). The variations in cell wall composition result in variable FSs in cotton. And how the microfiber orientation affects the twist of the fibers will be the focus in our future research. We believe that the arrangement of the cortical microtubules can influence the cellulose alignment and the twisting of mature fibers ensures their strength via GhSPL1 degradation in developing fiber cells by GhUBX. In the cotton cultivars, the number of helix is positively correlated with FS (Figure S4). Further investigation is necessary to explore how GhSPL1 regulates the cortical microtubule alignment or microfiber orientation and influences fiber twisting and SCW thickness.

Short tandem repeat variation in *GhUBX* correlates with the FS

SSRs are widespread in eukaryotic genomes as short tandem reiterations of sequence motifs. In recent years, there have been an increasing number of reports on their effects on a variety of complex traits (Hammock and Young, 2005). Many debilitating diseases are caused by the repeat expansions in noncoding regions of their resident genes including Huntington disease and hereditary ataxias (Fondon and Garner, 2004; Gatchel and Zoghbi, 2005; Mirkin, 2007; Fotsing et al., 2019). In plants, SSRs are widely used in marker-assisted breeding. The roles of the number of SSR units in regulating phenotypes have

been reported in multiple recent studies. For example, microsatellites in starch-synthesizing genes have been found in relation to starch physicochemical properties in waxy rice and 18 types of microsatellites, SNPs, and sequence-tagged sites at three genes are related to starch synthesis (Bao et al., 2002, 2006). A $(CT)_n$ repeat length variation in 5′-UTR of the *CaIMP* gene might regulate phytic acid levels to confer drought tolerance in natural populations of chickpeas (Joshi-Saha and Reddy, 2015). Also, a polymorphic $(GA/CT)_n$ varying motif difference of the tryptophan decarboxylase gene at 5′UTR could influence promoter activity (Kumar and Bhatia, 2016). More recently, a variation of specific microsatellite motif size and type enriched in differentially expressed transcripts among latitudinal populations of the common sunflower is reported (Ranathunge et al., 2018).

In *GhUBX*, there are three conservative domains: UBA-like, UAS, and UBX, and a 6-bp deletion located outside of these three domains (Figure S2E). Our present study has identified two classes of multiple microsatellite alleles, based on the nucleotide difference between cotton accessions $CTCGGCCTCT(GCCTCC)_{5/6}$, which were widely exited throughout the genome of *G. hirsutum*, this was authenticated by the microsatellite genotyping of 268 cultivars and RILs with K222 (Figures S2B and S2C). The correlation analysis suggested that *GhUBX* was significantly associated with FS (Figure S2). The overexpressed transgenic lines demonstrated a high-FS phenotype (Figure 2B and Table S7) and confirmed that *GhUBX* associated with FS significantly.

In summary, we cloned the causal gene, *GhUBX,* underlying the major FS QTL *qFS-D3-1*, through map-based cloning in cotton. GhUBX interacts with GhSPL1 and results in significantly increased FS in transgenic cotton. Moreover, GhUBX can act as a bridge between ubiquitin and GhSPL1 and reduce the GhSPL1 content in fiber cells via the ubiquitin 26S–proteasome pathway (Figure 5). The illustration of FS formation mechanism could enhance our understanding of fiber development theoretically and lay a foundation for improving fiber quality. How GhUBX regulates SCW directly and/or GhUBX interacts with other unknown proteins to influence SCW remains to be elucidated.

Limitations of the study

To further verify our results in natural populations, we tried to use InDel GWAS analysis to obtain the correlation between 6-bp InDel within GhUBX and FS, no significant peaks for FS were identified on Chr. D03. We also found that genotyping results based on PCR and Sanger sequencing were not consistent with the haplotypes as determined by resequencing data, indicating a high error of genotyping based on low-coverage resequencing data. For now, InDel markers are nearly used in GWAS analysis because of the high prevalence of false positives in InDels identified from low-coverage short-read sequencing.

STAR★METHODS

Detailed methods are provided in the online version of this paper and include the following:

- KEY RESOURCES TABLE
- RESOURCE AVAILABILITY
  - Lead contact
  - Materials availability
  - Data and code availability
- EXPERIMENTAL MODEL AND SUBJECT DETAILS
  - Plant materials
- METHODS DETAILS
  - Mapping population development and fiber quality measurement
  - Marker analysis and genetic map construction
  - The quantitative RT-PCR analysis
  - Scanning and transmission electron microscope analysis
  - Cotton transformation
  - Subcellular localization
  - Yeast two-hybrid assays and yeast three-hybrid assays
  - Pull-down assays
  - GhUBX polyclonal antibody preparation
  - Co-immunoprecipitation assays
  - Luciferase imaging assays

- BiFC assays
- Virus-induced gene silencing (VIGS) assay
- *In vitro* ubiquitination
- *In vitro*, *in vivo*, and semi–*in vivo* protein degradation assays
- Association mapping

- QUANTIFICATION AND STATISTICAL ANALYSIS

SUPPLEMENTAL INFORMATION

Supplemental information can be found online at https://doi.org/10.1016/j.isci.2021.102930.

ACKNOWLEDGMENTS

This study was financially supported by grants from the National Natural Science Foundation of China (31822036; 31701469); the National Research and Development Project of Transgenic Crops of China (2016ZX08009-003); the Fundamental Research Funds for the Central Universities (2019XZZX004-03, 2019XZZX004-13); and Leading Innovative and Entrepreneur Team Introduction Program of Zhejiang (2019R01002). We would like to thank the Bio-ultrastructure Analysis Lab. of the Analysis center of Agrobiology and Environmental Sciences, Zhejiang Univ. for the TEM and SEM assays.

AUTHOR CONTRIBUTIONS

T.Z. and Y.Z. designed the research; Y.Z., C.X., W.S., Y.W., Z.N., S.W, Z.H., Z.S., Y.Z., and L.F. performed experiments; T.Z., Y.Z., Y.H., and Y.W. analyzed the data; T.Z. and Y.Z. wrote the paper. All authors discussed results and commented on the manuscript.

DECLARATION OF INTERESTS

The authors declare no competing financial interests.

Received: January 17, 2021
Revised: July 9, 2021
Accepted: July 27, 2021
Published: August 20, 2021

REFERENCES

Bao, S., Corke, H., and Sun, M. (2002). Microsatellites in starch-synthesizing genes in relation to starch physicochemical properties in waxy rice (*Oryza sativa L.*). Theor. Appl. Genet. *105*, 898–905.

Bao, S., Corke, H., and Sun, M. (2006). Microsatellites, single nucleotide polymorphisms and a sequence tagged site in starch-synthesizing genes in relation to starch physicochemical properties in nonwaxy rice (*Oryza sativa* L.). Theor. Appl. Genet. *113*, 1185–1196.

Baskin, T.I. (2005). Anisotropic expansion of the plant cell wall. Annu. Rev. Cell Dev. Biol. *21*, 203–222.

Basten, C.J., Weir, B.S., and Zeng, Z.B. (2001). QTL Cartographer, Version 1.15 (Department of Statistics, North Carolina State University).

Burkart, G.M., and Dixit, R. (2019). Microtubule bundling by MAP65-1 protects against severing by inhibiting the binding of katanin. Mol. Biol. Cell *30*, 1587–1597.

Cao, J.F., Zhao, B., Huang, C.C., Chen, Z.W., Zhao, T., Liu, H.R., Hu, G.J., Shangguan, X.X., Shan, C.M., Wang, L.J., et al. (2020). The miR319-targeted GhTCP4 promotes the transition from cell elongation to wall thickening in cotton fiber. Mol. Plant *13*, 1063–1077.

Confraria, A., and Baena-González, E. (2016). Using *Arabidopsis* protoplasts to study cellular responses to environmental stress. Methods Mol. Biol. *1398*, 247–269.

Deruyffelaere, C., Purkrtova, Z., Bouchez, I., Collet, B., Cacas, J.L., Chardot, T., Gallois, J.L., and D'Andrea, S. (2018). PUX10 is a CDC48A adaptor protein that regulates the extraction of ubiquitinated oleosins from seed lipid droplets in *Arabidopsis*. Plant Cell *30*, 2116–2136.

Dumais, J., and Forterre, Y. (2012). "Vegetable Dynamicks": the role of water in plant movements. Annu. Rev. Fluid Mech. *44*, 453–478.

Fang, L., Wang, Q., Hu, Y., Jia, Y., Chen, J., Liu, B., Zhang, Z., Guan, X., Chen, S., Zhou, B., et al. (2017). Genomic analyses in cotton identify signatures of selection and loci associated with fiber quality and yield traits. Nat. Genet. *49*, 1089–1098.

Feng, H., Li, X., Chen, H., Deng, J., Zhang, C., Liu, J., Wang, T., Zhang, X., and Dong, J. (2018). GhHUB2, a ubiquitin ligase, is involved in cotton fiber development *via* the ubiquitin-26S proteasome pathway. J. Exp. Bot. *69*, 5059–5075.

Fondon, J.W., 3rd, and Garner, H.R. (2004). Molecular origins of rapid and continuous morphological evolution. Proc. Natl. Acad. Sci. USA *101*, 18058–18063.

Fotsing, S.F., Margoliash, J., Wang, C., Saini, S., Yanicky, R., Shleizer-Burko, S., Goren, A., and Gymrek, M. (2019). The impact of short tandem repeat variation on gene expression. Nat. Genet. *51*, 1652–1659.

Galva, C., Kirik, V., Lindeboom, J.J., Kaloriti, D., Rancour, D.M., Hussey, P.J., Bednarek, S.Y., Ehrhardt, D.W., and Sedbrook, J.C. (2014). The microtubule plus-end tracking proteins SPR1 and EB1b interact to maintain polar cell elongation and directional organ growth in *Arabidopsis*. Plant Cell *26*, 4409–4425.

Gao, X., Britt, R.C., Jr., Shan, L., and He, P. (2011). *Agrobacterium*-mediated virus-induced gene silencing assay in cotton. J. Vis. Exp. *54*, e2938.

Gatchel, J.R., and Zoghbi, H.Y. (2005). Diseases of unstable repeat expansion: mechanisms and common principles. Nat. Rev. Genet. *6*, 743–755.

Gong, S.Y., Huang, G.Q., Sun, X., Qin, L.X., Li, Y., Zhou, L., and Li, X.B. (2014). Cotton KNL1, encoding a class II KNOX transcription factor, is

involved in regulation of fibre development. J. Exp. Bot. *65*, 4133–4147.

Haigler, C.H. (2010). Physiological and anatomical factors determining fiber structure and utility. In Physiology of Cotton, J.M. Stewart, D. Oosterhuis, J.J. Heitholt, and J.R. Mauney, eds. (Springer Science+Business Media), pp. 33–47, Chapter 4.

Hammock, E.A., and Young, L.J. (2005). Microsatellite instability generates diversity in brain and sociobehavioral traits. Science *308*, 1630–1634.

Han, L.B., Li, Y.B., Wang, H.Y., Wu, X.M., Li, C.L., Luo, M., Wu, S.J., Kong, Z.S., Pei, Y., Jiao, G.L., et al. (2013). The dual functions of WLIM1a in cell elongation and secondary wall formation in developing cotton fibers. Plant Cell *25*, 4421–4438.

Hsieh, Y.L. (1999). Structural development of cotton fibers and linkages to fiber quality. In Cotton Fibers, A.S. Basra, ed. (Binghampton: Food Products Press), pp. 137–166.

Hu, Y., Chen, J., Fang, L., Zhang, Z., Ma, W., Niu, Y., Ju, L., Deng, J., Zhao, T., Lian, J., et al. (2019). *Gossypium barbadense* and *Gossypium hirsutum* genomes provide insights into the origin and evolution of allotetraploid cotton. Nat. Genet. *51*, 739–748.

Huang, J., Guo, Y., Sun, Q., Zeng, W., Li, J., Li, X., and Xu, W. (2019). Genome-wide identification of R2R3-MYB transcription factors regulating secondary cell wall thickening in cotton fiber development. Plant Cell Physiol. *60*, 687–701.

Ishida, T., Thitamadee, S., and Hashimoto, T. (2007). Twisted growth and organization of cortical microtubules. J. Plant Res. *120*, 61–70.

Jaffe, M.J., and Galston, A.W. (1968). The physiology of tendrils. Annu. Rev. Plant Physiol. *19*, 417–434.

Jian, G., Ma, C., and Zheng, C. (2003). Advances in cotton breeding for resistance to fusarium and verticillium wilt in the last fifty years in China. Agr. Sci. China *2*, 280–288.

Joshi-Saha, A., and Reddy, K.S. (2015). Repeat length variation in the 5′UTR of myo-inositol monophosphatase gene is related to phytic acid content and contributes to drought tolerance in chickpea (*Cicer arietinum L.*). J. Exp. Bot. *66*, 5683–5690.

Kong, L., Cheng, J., Zhu, Y., Ding, Y., Meng, J., Chen, Z., Xie, Q., Guo, Y., Li, J., Yang, S., et al. (2015). Degradation of the ABA co-receptor ABI1 by PUB12/13 U-box E3 ligases. Nat. Commun. *6*, 8630.

Kretzschmar, F.K., Mengel, L.A., Muller, A.O., Schmitt, K., Blersch, K.F., Valerius, O., Braus, G.H., and Ischebeck, T. (2018). PUX10 is a lipid droplet-localized scaffold protein that interacts with CELL DIVISION CYCLE48 and is involved in the degradation of lipid droplet proteins. Plant Cell *30*, 2137–2160.

Kumar, S., and Bhatia, S. (2016). A polymorphic (GA/CT)n- SSR influences promoter activity of tryptophan decarboxylase gene in *Catharanthus roseus L. Don*. Sci. Rep. *6*, 33280.

Lacape, J.M., Llewellyn, D., Jacobs, J., Arioli, T., Becker, D., Calhoun, S., Al-Ghazi, Y., Liu, S., Palai, O., Georges, S., et al. (2010). Meta-analysis of cotton fiber quality QTLs across diverse environments in a *Gossypium hirsutum* x *G. barbadense* RIL population. BMC Plant Biol. *10*, 132.

Lee, Y., Chou, T., Pittman, S.K., Keith, A.L., Razani, B., and Weihl, C.C. (2017). Keap1/Cullin3 modulates p62/SQSTM1 activity *via* UBA domain ubiquitination. Cell Rep. *19*, 188–202.

Li, F., Wu, S., Lü, F., Chen, T., Ju, M., Wang, H., Jiang, Y., Zhang, J., Guo, W., and Zhang, T. (2009). Modified fiber qualities of the transgenic cotton expressing a silkworm fibroin gene. Chin. Sci. Bull. *54*, 1210–1216.

Li, H., Sun, B., Sasabe, M., Deng, X., Machida, Y., Lin, H., Julie Lee, Y.R., and Liu, B. (2017). *Arabidopsis* MAP65-4 plays a role in phragmoplast microtubule organization and marks the cortical cell division site. New Phytol. *215*, 187–201.

Li, Y., Wang, N.N., Wang, Y., Liu, D., Gao, Y., Li, L., and Li, X.B. (2018). The cotton XLIM protein (GhXLIM6) is required for fiber development *via* maintaining dynamic F-actin cytoskeleton and modulating cellulose biosynthesis. Plant J. *96*, 1269–1282.

Liu, L., Zhang, Y., Tang, S., Zhao, Q., Zhang, Z., Zhang, H., Dong, L., Guo, H., and Xie, Q. (2010). An efficient system to detect protein ubiquitination by agroinfiltration in *Nicotiana benthamiana*. Plant J. *61*, 893–903.

Livak, K.J., and Schmittgen, T.D. (2001). Analysis of relative gene expression data using real-time quantitative PCR and the 2(-Delta Delta C(T)) Method. Methods *25*, 402–408.

Lucas, J.R., and Shaw, S.L. (2012). MAP65-1 and MAP65-2 promote cell proliferation and axial growth in *Arabidopsis* roots. Plant J. *71*, 454–463.

Ma, Q., Wang, N., Hao, P., Sun, H., Wang, C., Ma, L., Wang, H., Zhang, X., Wei, H., and Yu, S. (2019). Genome-wide identification and characterization of TALE superfamily genes in cotton reveals their functions in regulating secondary cell wall biosynthesis. BMC Plant Biol. *19*, 432.

Martinez-Sanz, M., Pettolino, F., Flanagan, B., Gidley, M.J., and Gilbert, E.P. (2017). Structure of cellulose microfibrils in mature cotton fibres. Carbohydr. Polym. *175*, 450–463.

McCouch, S.R., Chen, X., Panaud, O., Temnykh, S., Xu, Y., Cho, Y.G., Huang, N., Ishii, T., and Blair, M. (1997). Microsatellite marker development, mapping and applications in rice genetics and breeding. Plant Mol. Biol. *35*, 89–99.

Mei, M., Syed, N.H., Gao, W., Thaxton, P.M., Smith, C.W., Stelly, D.M., and Chen, Z.J. (2004). Genetic mapping and QTL analysis of fiber-related traits in cotton (*Gossypium*). Theor. Appl. Genet. *108*, 280–291.

Mirkin, S.M. (2007). Expandable DNA repeats and human disease. Nature *447*, 932–940.

Nakajima, K., Furutani, I., Tachimoto, H., Matsubara, H., and Hashimoto, T. (2004). SPIRAL1 encodes a plant-specific microtubule-localized protein required for directional control of rapidly expanding *Arabidopsis* cells. Plant Cell *16*, 1178–1190.

Neuber, O., Jarosch, E., Volkwein, C., Walter, J., and Sommer, T. (2005). Ubx2 links the Cdc48 complex to ER-associated protein degradation. Nat. Cell Biol. *7*, 993–998.

Ning, Z., Chen, H., Mei, H., and Zhang, T. (2014). Molecular tagging of QTLs for fiber quality and yield in the upland cotton cultivar Acala-Prema. Euphytica *195*, 143–156.

Ooijen, J., and Voorrips, R.E. (2001). JoinMap version 3.0: software for the calculation of genetic linkage maps. CPRO-DLO, Wageningen, The Netherlands.

Paredez, A.R., Somerville, C.R., and Ehrhardt, D.W. (2006). Visualization of cellulose synthase demonstrates functional association with microtubules. Science *312*, 1491–1495.

Paterson, A.H., Brubaker, C.L., and Wendel, J.F. (1993). A rapid method for extraction of cotton (*Gossypium spp.*) genomic DNA suitable for RFLP or PCR analysis. Plant Mol. Biol. Rep. *11*, 122–127.

Qin, Z., Bai, Y., Muhammad, S., Wu, X., Deng, P., Wu, J., An, H., and Wu, L. (2019). Divergent roles of FT-like 9 in flowering transition under different day lengths in *Brachypodium distachyon*. Nat. Commun. *10*, 812.

Ranathunge, C., Wheeler, G.L., Chimahusky, M.E., Kennedy, M.M., Morrison, J.I., Baldwin, B.S., Perkins, A.D., and Welch, M.E. (2018). Transcriptome profiles of sunflower reveal the potential role of microsatellites in gene expression divergence. Mol. Ecol. *27*, 1188–1199.

Rong, J., Feltus, F.A., Waghmare, V.N., Pierce, G.J., Chee, P.W., Draye, X., Saranga, Y., Wright, R.J., Wilkins, T.A., May, O.L., et al. (2007). Meta-analysis of polyploid cotton QTL shows unequal contributions of subgenomes to a complex network of genes and gene clusters implicated in lint fiber development. Genetics *176*, 2577–2588.

Sambade, A., Findlay, K., Schäffner, A.R., Lloyd, C.W., and Buschmann, H. (2014). Actin-dependent and -independent functions of cortical microtubules in the differentiation of *Arabidopsis* leaf trichomes. Plant Cell *26*, 1629–1644.

Schuberth, C., and Buchberger, A. (2005). Membrane-bound Ubx2 recruits Cdc48 to ubiquitin ligases and their substrates to ensure efficient ER-associated protein degradation. Nat. Cell Biol. *7*, 999–1006.

Sedbrook, J.C., Ehrhardt, D.W., Fisher, S.E., Scheible, W.R., and Somerville, C.R. (2004). The *Arabidopsis* sku6/spiral1 gene encodes a plus end-localized microtubule-interacting protein involved in directional cell expansion. Plant Cell *16*, 1506–1520.

Shoji, T., Narita, N.N., Hayashi, K., Asada, J., Hamada, T., Sonobe, S., Nakajima, K., and Hashimoto, T. (2004). Plant-specific microtubule-associated protein SPIRAL2 is required for anisotropic growth in *Arabidopsis*. Plant Physiol. *136*, 3933–3944.

Skotheim, J.M., and Mahadevan, L. (2005). Physical limits and design principles for plant and fungal movements. Science *308*, 1308–1310.

Smyth, D.R. (2016). Helical growth in plant organs: mechanisms and significance. Development *143*, 3272–3282.

Sun, Q., Huang, J., Guo, Y., Yang, M., Guo, Y., Li, J., Zhang, J., and Xu, W. (2020). A cotton NAC domain transcription factor, GhFSN5, negatively regulates secondary cell wall biosynthesis and anther development in transgenic *Arabidopsis*. Plant Physiol. Bioch. *146*, 303–314.

Tiwari, S.C., and Wilkins, T.A. (1995). Cotton (*Gossypium hirsutum*) seed trichomes expand via diffuse growing mechanism. Can. J. Bot. *73*, 746–775.

Ulloa, M., and Wrjr, M. (2000). Genetic linkage map and QTL analysis of agronomic and fiber quality traits in an intraspecific population. J. Cotton Sci. *4*, 161–170.

Varshavsky, A. (2017). The ubiquitin system, autophagy, and regulated protein degradation. Annu. Rev. Biochem. *86*, 123–128.

Voorrips, R.E. (2002). MapChart 2.2: software for the graphical presentation of linkage maps and QTLs. J. Hered. *93*, 77–78.

Wang, S., Kurepa, J., Hashimoto, T., and Smalle, J.A. (2011). Salt stress-induced disassembly of *Arabidopsis* cortical microtubule arrays involves 26S proteasome-dependent degradation of SPIRAL1. Plant Cell *23*, 3412–3427.

Wang, Y., Ning, Z., Hu, Y., Chen, J., Zhao, R., Chen, H., Ai, N., Guo, W., and Zhang, T. (2015). Molecular mapping of restriction-site associated DNA markers in allotetraploid upland cotton. PLoS One *10*, e0124781.

Wu, S., Wang, H., Li, F., Chen, T., Zhang, J., Jiang, Y., Ding, Y., Guo, W., and Zhang, T. (2008). Enhanced agrobacterium-mediated transformation of embryogenic calli of upland cotton via efficient selection and timely subculture of somatic embryos. Plant Mol. Biol. Rep. *26*, 174–185.

Xia, T., Li, N., Dumenil, J., Li, J., Kamenski, A., Bevan, M.W., Gao, F., and Li, Y. (2013). The ubiquitin receptor DA1 interacts with the E3 ubiquitin ligase DA2 to regulate seed and organ size in *Arabidopsis*. Plant Cell *25*, 3347–3359.

Yanagisawa, M., Desyatova, A.S., Belteton, S.A., Mallery, E.L., Turner, J.A., and Szymanski, D.B. (2015). Patterning mechanisms of cytoskeletal and cell wall systems during leaf trichome morphogenesis. Nat. Plants *1*, 15014.

Yang, Y., Fu, D., Zhu, C., He, Y., Zhang, H., Liu, T., Li, X., and Wu, C. (2015). The RING-Finger ubiquitin ligase HAF1 mediates heading date 1 degradation during photoperiodic flowering in rice. Plant Cell *27*, 2455–2468.

Zhang, T., Yuan, Y., Yu, J., Guo, W., and Kohel, R.J. (2003). Molecular tagging of a major QTL for fiber strength in upland cotton and its marker-assisted selection. Theor. Appl. Genet. *106*, 262–268.

Zhang, M., Yu, Q., Liu, Z., Liang, C., Zhang, B., and Li, M. (2017). UBX domain-containing proteins are involved in lipid homeostasis and stress responses in *Pichia pastoris*. Int. J. Biochem. Cell Biol. *90*, 136–144.

Zhang, J., Huang, G.Q., Zou, D., Yan, J.Q., Li, Y., Hu, S., and Li, X.B. (2018). The cotton (*Gossypium hirsutum*) NAC transcription factor (FSN1) as a positive regulator participates in controlling secondary cell wall biosynthesis and modification of fibers. New Phytol. *217*, 625–640.

STAR★METHODS

KEY RESOURCES TABLE

REAGENT or RESOURCE	SOURCE	IDENTIFIER
Antibodies		
Anti-His	Sigma-Aldrich	Cat# SAB1305538; RRID: AB_2687993
Anti-GST	Sigma-Aldrich	Cat# G7781, RRID:AB_259965
Anti-GFP	Sigma-Aldrich	Cat # G1546; RRID: AB_1079024
Anti-RFP	Sigma-Aldrich	Cat# AB3528, RRID:AB_91496
Bacterial and Virus Strains		
Trelief ™ 5α Chemically Competent Cell (DH5a)	Tsingke	Cat# TSC01
GV3101(pSoup) Chemically Competent Cell	WeidiBio	CAT#: AC1002
EHA105 Electroporation-Competent Cell	WeidiBio	CAT#: AE1010
Chemicals, Peptides, and Recombinant Proteins		
Murashige and Skoog Basal Medium	Sigma-Aldrich	M5519
MG132	Sigma-Aldrich	Cat#M8699-1MG
$MgCl_2.6H_2O$	SIGMA	M2670
MES	SIGMA	M8250
$CaCl_2$	SIGMA	C5670
Kanamycin sulfate	Amresco	0408
Rifampicin	SIGMA	R3501
Ampicillin	Amresco	0399
Silwet L-77	GE Healthcare	SL77080596
Dimethyl sulfoxide	SIGMA	D8418
PMSF	American Bioanalytical	AB01620
cOmplete, Protease Inhibitor Cocktail	Sigma-Aldrich	Cat#4693159001
Critical Commercial Assays		
Scanning and transmission electron microscope analysis	Bio-ultrastructure Analysis Laboratory of the Analysis Center, Agrobiology and Environmental Sciences, Zhejiang University	NA
Cotton transformation	Biotechnology Research Center, Shanxi Academy of Agricultural Sciences	NA
Fiber quality measurement	Cotton Quality Supervision, Inspection and Testing Center, Ministry of Agriculture, Xinjiang, China.	NA
Experimental Models: Organisms/Strains		
TM-1	This paper	NA
Prema	This paper	NA
86-1	This paper	NA
W0	This paper	NA
N. benthamiana	This paper	NA
Arabidopsis thaliana ecotypes Col-0 and Ler	This paper	NA
Arabidopsis thaliana: *spiral1*	ABRC	SALK_048697
Arabidopsis thaliana: *spiral1-1*	ABRC	CS6546

(*Continued on next page*)

Continued

REAGENT or RESOURCE	SOURCE	IDENTIFIER
Oligonucleotides		
Primers are listed in Table S1	This paper	NA
Recombinant DNA		
35S::GhUBX-86-1-GST	This paper	NA
35S::GhUBX-Prema-GST	This paper	NA
35S::GhSPL1-HIS	This paper	NA
35S::GhSPL1-RFP	This paper	NA
35S::GhUBX-Prema-GFP	This paper	NA
35S::GhUBX-86-1-GFP	This paper	NA
35S::MAP65-RFP	Li et al.,2017	NA
Software and Algorithms		
Prism 6	https://www.graphpad.com/	NA
ImageJ	https://imagej.net/Welcome	NA

RESOURCE AVAILABILITY

Lead contact

Further information and requests for resources and reagents should be directed to and will be fulfilled by the Lead Contact, Tianzhen Zhang (cotton@njau.edu.cn).

Materials availability

All materials are available after completion of the respective material transfer agreements.

Data and code availability

Any data information reported in this paper is available from the lead contact upon request.

This study did not generate new reagents or software code.

EXPERIMENTAL MODEL AND SUBJECT DETAILS

Plant materials

Upland cotton (*Gossypium hirsutum*) plants, W0, TM-1, Prema, and 86-1, were cultivated in the field at the experimental station of Nanjing Agricultural University (NJAU) in China. The high–fiber strength parental line Prema, developed in California by a cross (AXTE-1 × NM49-2) × (C6TE × NMB3080), is a high–fiber quality Acala cultivar (Ulloa and WrJr, 2000). Prema was an introgressed line from *Gossypium thurberi* and *Gossypium barbadense*. The low–fiber strength parental line 86-1 had been widely cultivated in the Yangtze River and Yellow River cotton growing regions since the 1980s (Jian et al., 2003). In 2005, Prema and 86-1 were crossed at the Jiangpu Breeding Station, Nanjing Agricultural University (JBS/NAU), and RIL families were constructed and used for the present research (Ning et al., 2014). RILs were planted in China at Jiangpu, Nanjing/Jiangsu, Sanya/Hainan, and Shihezi/Xinjiang in 2009 and in Shihezi/Xinjiang and Dafeng/Jiangsu in 2010. Fiber cells at different developmental stages were carefully removed from seeds and immediately snap-frozen in liquid nitrogen for DNA and RNA extraction.

METHODS DETAILS

Mapping population development and fiber quality measurement

According to the genotype and location of the QTL mapped on the RILs population (Acala Prema × 86-1), we selected four RILs: RIL168, RIL98, RIL120, RIL43, which with fine fiber strength in diverse environments for years to cross with 86-1 in the summer of 2014 at the JBS/NAU. The F_1 plants were self-pollinated in the winter of 2014 in Hainan Island to produce F_2 progeny. A total of 1864 F_2 individuals, including four F_2 populations were planted in the summer of 2015 in JBS/NAU, the sample size of each F_2 populations crossed between RIL168, RIL98, RIL120 and RIL43, and 86-1 was 747, 355, 417 and 345 individuals, respectively. All

naturally opened bolls were hand-harvested to gain fiber that could be measured for fiber quality, including fiber length (FL, mm), strength (FS, cN/tex), micronaire (FMIC), elongation (FE), and uniformity ratio (FU). Leaf samples were collected from 6-week-old plants of each F_2 generation grown in the field.

For comparative field trials, the transgenic cotton and WT were planted in a randomized block design with three replications. Each experimental replication included approximately one 4.5-m long row, with 75 cm between rows and 35 cm between plants in each row. Five plants in the middle of each row were tagged for harvesting. The middle cotton bolls were harvested and the fiber quality was investigated. Fiber quality traits included the FL, FS, FMIC, FE, and FU. The testing standard was the GB/T 20392-2006 HVI Cotton Fiber Physical Properties Test Method. Fiber samples were measured by the Cotton Quality Supervision, Inspection and Testing Center, Ministry of Agriculture, Xinjiang, China.

Marker analysis and genetic map construction

Cotton genomic DNA was extracted from young leaves using a modified cetyl trimethylammoniun bromide method (Paterson et al. 1993). To enrich markers within the QTL region, SNP markers identified by restriction site–associated DNA sequencing and InDel markers identified by transcriptome sequencing were used for fine mapping (Wang et al., 2015). SSR and InDel markers were developed based on the resequencing data between 86-1 and Prema. The markers used in the present research are listed in Table S1. Primers were synthesized by TSINGKE (Beijing, China) and mapped on Chr. D03, which displayed a clear polymorphism between two parents. Joinmap3.0 (Ooijen and Voorrips, 2001) was used to construct the genetic map of the primary QTL region on Chr. D03, with a LOD score of 6.0 and a recombination frequency of 0.40. The complex interval mapping method of Windows QTL Cartographer 2.5 (Basten et al., 2001) was used to identify the QTL for the fiber quality traits. QTLs were determined to be significant if the corresponding likelihood ratio score was greater than 11.5. MapChart2.2 (Voorrips, 2002) was used to develop the linkage group and anchor the QTL. The QTL was named starting with q, followed by an abbreviation of the trait name, the name of the chromosome, and the QTL number affecting the trait on the chromosome (QTL + trait + number) (McCouch et al., 1997).

The quantitative RT-PCR analysis

The qRT-PCR specific primers were designed using Integrated DNA Technologies online (https://sg.idtdna.com). *Histone3* (AF024716) was used as an internal control. qRT-PCR was carried out on an Applied Biosystems 7500 Fast Real-Time PCR System (Life Technologies, Foster City, CA, USA) in a 20-μl volume containing 100 ng of cDNA, 4 pM of each primer, and 10 μl of AceQ qPCR SYBR Green Master Mix (Vazyme, Nanjing, China) according to the manufacturer's protocol. The data were evaluated using the comparative cycle threshold method described by Livak and Schmittgen (Livak and Schmittgen, 2001). Three biological replicates (three samples harvested from three plants, one from each) were performed per reaction, each with two technical replicates (using the same sample). Mean values and standard errors were calculated according to the data from three replicates.

Scanning and transmission electron microscope analysis

Samples of mature fibers from Prema, 86-1, transgenic cotton lines, and W0 were dehydrated, fixed on the observation table, sputter-coated with silver using an E-1010/E-1020 ion sputter (Hitachi, Japan), and imaged using an SU8010 scanning electron microscope at 3.0 kV (Hitachi, Japan).

The mature fibers of the transgenic cotton were observed using a transmission electron microscope. Transverse sections of the fiber samples were fixed in 2.5% glutaraldehyde in a phosphate buffer overnight at 4°C and then in 1% OsO_4 for 2 hours. The samples were further dehydrated through the application of step-graded ethanol and embedded in Spurr's medium prior to ultrathin sectioning. Sections (90 nm thick) were cut with an ultramicrotome (EMUC7, 645 Leica, Germany) and collected on nickel mesh. The sections were air dried, stained, and viewed with a Hitachi H-7650 TEM at 80 kV (Bio-ultrastructure Analysis Laboratory of the Analysis Center of Agrobiology and Environmental Sciences, Zhejiang University). Five to 10 nonserial sections per genotype from fibers were examined per line. At least 10 cell wall interfaces between the fiber and fiber base from fibers per genotype were examined. The same mature fiber samples used for fiber quality investigation were also used for scanning and transmission electron microscopic analysis.

Cotton transformation

For the overexpression constructs, primers with added *Bam*H I and *Sma* I, were used to amplify the open reading frame of GhUBX from 86-1, which was then cloned into the pBI121 vector under the control of the constitutive cauliflower mosaic virus 35S promoter. GhUBX-overexpression (GhUBX-OE) construct was introduced into *G. hirsutum acc.* W0 via *Agrobacterium tumefaciens*–mediated transformation. Agrobacterium strain LBA4404 holding the pBI121 plasmid vector was grown in Luria–Bertani liquid medium supplemented with 50 mg/L kanamycin and 10 mg/L rifampicin at 28°C for 24 h. The bacteria were resuspended in liquid MSB_1 medium and the standard OD600 was adjusted to 0.3~0.5. Embryogenic calli were inoculated with the *Agrobacterium* suspension for 20 min and subsequently blotted dry with sterile filter papers. Then, the calli were dispersed and cocultured on MSB_1 medium placed on filter paper in the dark (Wu et al., 2008). The homozygosity of the transgenic plants was determined using the kanamycin selection marker coupled with PCR-based genotyping. DNA polymerase ($I5^{TM}$ 2 × High-Fidelity Master Mix) was purchased from TSINGKE (Beijing, China). The primers used for vector construction and PCR-based screening were listed in Table S1.

Subcellular localization

For subcellular localization of *GhUBX* in *N. benthamiana* leaves, the coding sequence of GhUBX was cloned into the vector pBinGFP4 to form GhUBX-GFP.*A. tumefaciens* strain GV3101 carrying the construct was used to infiltrate 6-week-old *N. benthamiana* leaves. For the subcellular location of *GhUBX* and *MAP-65* in *Arabidopsis* protoplast, the *GhUBX*-GFP4 and *MAP-65* plasmid were transiently transformed via PEG/Ca^{2+} and conducted as previously reported (Confraria and Baena-González, 2016). *MAP-65* used as microtubule marker (Lucas and Shaw, 2012; Li et al., 2017). Analysis was performed on a Zeiss LSM780 confocal microscope using a 488-nm excitation laser for GFP and a 561-nm laser for RFP. Images were processed using Zen 2009 software.

Yeast two-hybrid assays and yeast three-hybrid assays

The yeast two-hybrid (Y2H) assay was performed using the Gal4 vector system (Clontech, USA). Sectionalized GhUBX and GhSPL1 were cloned into both the pGBKT7 vector and pGADT7 vector. The coding regions of GhUBX (86-1-1-472), GhUBX (Prema-1-470), GhUBX (153-472) (non-distinctive region), GhUBX (86-1-1-83), GhUBX (Prema-1-81), GhUBX (86-1-71-153), GhUBX (Prema-71-153), GhUBX (1-50) (non-distinctive region), and GhSPL1 were cloned into both the pGBKT7 vector and pGADT7 vector, respectively. The constructs were cotransformed into yeast strain Y2H. The transformed cells were adjusted to OD600 = 0.4 ~ 0.6 and grown in SD/-Trp-Leu or SD/-Trp-Leu-His-Ade plates for 3 to 7 days at 30°C.

Y3H assay was performed based on the pBridge vector system (Takara Bio, Japan). The conserved ubiquitin sequence was fused to GAL4 AD in pGADT7. To construct the pBridge-GhSPL1-GhUBX, the full-length coding sequence of the GhSPL1 coding region was cloned into multiple cloning site (MCS) I of the pBridge vector fused to the GAL4 BD domain, and the sectionalized GhUBX coding region was cloned into MCS II of the pBridge vector. The transformed cells were grown in SD/-Trp-Leu-Met plates and SD/-Trp-Leu-His-Met plates for 5 to 8 days at 30°C.

Pull-down assays

The coding sequences of GhUBX-Prema/86-1 and GhSPL1 were cloned into the pGEX-4T-1 vector and pET-32a vector to generate the constructs to express GST-GhUBX-Prema/86-1 and His-GhSPL1, respectively. The pull-down assays were performed in accordance with previous reported methods (Xia et al., 2013).

GhUBX polyclonal antibody preparation

For the preparation of the GhUBX polyclonal antibody, a 1416-bp coding-region fragment encoding a 472–amino acid peptide of GhUBX-86-1 was cloned into a pET32a vector (AOGENE, Nanjing, China). The recombinant protein was expressed in *Escherichia coli* DE3 (Transgen, Beijing, China) and purified to produce rabbit polyclonal antibodies (prepared by AOGENE of China).

Co-immunoprecipitation assays

Co-immunoprecipitation (co-IP) was conducted as previously described (Liu et al., 2010). In brief, *GhSPL1*-RFP and *GhUBX*-GFP or vector-GFP and vector-RFP were transiently co-expressed in *N. benthamiana*

leaves for 3 days. At 12 hours before sample collection, 100 μM of the 26S-proteasome inhibitor MG132 was infiltrated. Lysates were incubated with anti-GFP or anti-RFP affinity M2 beads (Sigma-Aldrich, St. Louis, MO, USA) at 4°C for 2 hours. The beads were washed three times with PBS, and the immunoprecipitated proteins were examined by immunoblotting (Ruiyuan Biotech, Nanjing, China).

Luciferase imaging assays

For the firefly LUC complementation imaging assays, the sectionalized sequences of GhUBX-P, GhUBX-8, GhUBX-P-1-153, GhUBX-8-1-153, and GhUBX-153-472 were respectively ligated with the N-terminal fragment of luciferase (nLUC) to form sectionalized-GhUBX-nLUC. The full-length coding sequences of GhSPL1 were fused with the C-terminal fragment of luciferase (cLUC). FT1 and FD worked as positive controls (Qin et al., 2019). The images were taken by a low-light, cooled, charge-coupled device imaging apparatus (Tanon, Fremont, CA, USA) (Kong et al., 2015).

BiFC assays

For the BiFC assays, sectionalized sequences of *GhUBX* were cloned into YNE and fused with the N-terminus of YFP; and *GhSP1L1* was cloned into YCE and fused with the C- terminus of YFP. The recombinant constructs were co-transformed in pairs into young *N. benthamiana* leaves, and *MAP65-RFP,* which served as a marker for the microtubule localization, was also co-transformed (Lucas and Shaw, 2012; Li et al., 2017; Burkart and Dixit, 2019). The fluorescence signal was observed using a Zeiss LSM780 confocal microscope.

Virus-induced gene silencing (VIGS) assay

For Virus-induced gene silencing (VIGS) assay, a 296-bp fragment of GhSPL1 cDNA, corresponding to bases 22 to 317 of the GhSPIRAL1-like1 gene, was amplified by PCR. The resulting PCR product was cloned into pTRV2 to produce a vector referred to as pTRV2-GhSPL1. *Agrobacterium* cells respectively carrying pTRV1 and pTRV2-GhSPL1 were re-suspended in an infiltration medium (10 mM $MgCl_2$, 10 mM MES, 200 μM acetosyringone) and adjusted to an OD600 of 1.0. The *Agrobacterium* strains containing the pTRV1 and pTRV2-GhSPL1 vectors were mixed at a ratio of 1:1. The *Agrobacterium* suspension was injected into the cotyledons of 10-day-old seedlings, which were placed in the dark for 24 hours and then incubated at 23°C with a 16-hour light/8-hour dark cycle. The TM-1 was used as a receptor to carry on the VIGS assay to silence the *GhSPL1* gene. Empty-vector (TRV: 00) transformed plants were used as experimental controls. The chloroplast alterados 1 (*CLA1*) gene was used as an indicating gene to control the silencing effect (Gao et al., 2011). Thirty seedlings were used as experimental groups to silence the *GhSPL1* gene. The photos were taken three weeks after injection, and leaves were collected for expression detection.

In vitro ubiquitination

GST-GhUBX-Prema/86-1 and His-GhSPL1 proteins were purified from the *E. coli* strain Arctic-Express. *In vitro* ubiquitination assay was conducted as previously reported (Yang et al., 2015).

In vitro, in vivo, and semi–*in vivo* protein degradation assays

In vitro degradation assays were performed in accordance with previously reported methods (Yang et al., 2015). For semi–*in vivo* protein degradation analysis, a GhUBX-Prema-GFP sample, GhUBX-86-1-GFP sample, GhSPL1-RFP sample, and GFP sample were harvested at 3 days after inoculation. The four samples were separately extracted with native extraction buffer (50 mM Tris-MES [pH 8.0], 0.5 M sucrose, 1 mM $MgCl_2$, 10 mM EDTA, 5 mM DTT, and a protease inhibitor cocktail (CompleteMini tablets; Roche, Indianapolis, IN, USA); the indicated concentrations of ATP, CHX, and MG132 or DMSO (control) were added to the protein extract. The mixtures were incubated at 25°C. Samples were removed at different time points for immunoblot analyses.

For *in vivo* degradation assays, we coinfiltrated the *Agrobacterium* strains carrying the *GhUBX* (Prema/86-1)-GFP and *GhSPL1*-RFP plasmids into *N. benthamiana* leaves for 3 days. The corresponding empty vectors were used as the controls, and the RFP plasmid was added as an internal control. For proteasome inhibition, leaves were infiltrated with a 10 mM $MgCl_2$ and 100 mM MG132 solution for 14 hours before sample collection. Samples were collected for protein and RNA extraction. For protein-level analysis, the extracts were analyzed using anti-GFP antibody (1:1000 dilution), anti-RFP antibody (1:1000 dilution),

anti-GhUBX antibody (1:1000 dilution), and anti-GhSPL1 antibody (1:1000 dilution). For RNA level expression analysis, RT-PCR was performed.

Association mapping

A haplotype association panel composed of 268 diverse cotton cultivars was used in the association analysis of the tandem repeats for GhUBX (Table S6). This association population was previously phenotyped for all fiber quality traits (Fang et al., 2017). The significance of difference was analyzed with two-tailed test. Another population composed of 486 cotton cultivars were used to analyze the association between fiber strength and helices number. 20 individuals with highest FS (cN/tex > 35) and 20 individuals with lowest FS (cN/tex < 26) were selected from this population and calculated their helices. The helices number and other fiber quality traits are shown in Table S8.

QUANTIFICATION AND STATISTICAL ANALYSIS

In this study, significant differences between two samples were determined with Two-tailed paired Student's t test. Error bars represent standard deviation of mean, 'n' represents the sample size, as mentioned in the figure legends. And asterisks indicate the statistical significance: *, $p < 0.05$; **, $p < 0.01$. At least three biological replicates were included. Statistical analysis was performed by GraphPad Prism 6.0. Thickness of cell wall was analysis by ImageJ.